GAMMA RADIATION FROM THE CRAB AND VELA PULSARS

Gottfried Kanbach

Max-Planck-Institut für Physik u. Astrophysik
Institut für Extraterrestrische Physik
D-8046 Garching, F.R.G.

ABSTRACT

The young pulsars in Crab and Vela have been observed as very efficient emitters of high energy gamma radiation. While their radiation in the radio-, optical- and X-ray range was always known to differ considerably, the gamma-ray emission on a superficial level appears quite similar:

- lightcurves with two narrow peaks, separated by 141° (Crab) and 153° (Vela)
- photon energies in excess of 1 GeV with spectra that can be described by a power-law for Crab and a broken power-law for Vela.

The detailed observations of these sources with the COS-B instrument, extending over nearly seven years, have revealed significant differences in the characteristics of the pulsars in the gamma-ray domain. Secular changes in the temporal (Crab) and spectral (Vela) properties above 50 MeV have been found. These tantalizing signatures of the pulsar emission processes must now be explored in more detail and over a larger spectral range with the GRO instruments in order to gain a deeper understanding of the physics of young neutron stars.

I. INTRODUCTION

The conventional model for a pulsar holds that all radiative emissions of such an object are powered by the loss of rotational energy of a neutron star:

$$\dot{E}_{rot} = 4\pi^2 I \dot{P} P^{-3}$$

If a part η (=efficiency) of this energy loss is transformed into high energy photons of an average energy $< E_\gamma >$ which are beamed into a solid angle Ω the observer at a distance d can register a photon flux of:

$$\phi = \frac{\dot{E}_{rot}\eta}{<E_\gamma>} \times \frac{1}{\Omega d^2}$$

while being illuminated by the beam. The time duty cycle β reduces the beam flux to the time average flux $< \phi >= \phi \times \beta$, which can be written in suitable units as:

$$< \phi >= 7 \times 10^{-9} I_{45} \dot{P}_{-15} P^{-3} \eta \beta \Omega^{-1} d_{kpc}^{-2} \;\; (\gamma > 100\ MeV)\ cm^{-2}\ s^{-1}$$

where I_{45} is the moment of inertia in units of $10^{45}\ g\ cm^2$

$\dot{P}_{-15}$ is the period change in $10^{-15}\ s/s$

P is the period in seconds.

The assumed gamma spectrum is proportional to E^{-2}. A pencil beam emission geometry and reasonable assumptions on I_{45} and distance lead to the following requirements for the efficiency η for the Crab and Vela pulsars:

Crab: $< \phi >= 2.6 \times 10^{-6}\ (\gamma > 100\ MeV)\ cm^{-2}\ s^{-1} \quad \rightarrow \quad \eta \approx 10^{-3}$

Vela: $< \phi >= 1.2 \times 10^{-5}\ (\gamma > 100\ MeV)\ cm^{-2}\ s^{-1} \quad \rightarrow \quad \eta \approx 10^{-2}$

Even allowing for some uncertainty in the assumed parameters, these efficiencies indicate a major energy loss process and show that gamma-ray observations probe the central high-energy engine of young pulsars.

II. THE CRAB PULSAR AND NEBULA

Gamma-ray observations of the galactic anticenter region with the instruments on SAS-2 (1972/73) and COS-B (1975-1982) have confirmed the Crab pulsar (PSR0531+21) as a strong source of high energy photons and have provided a detailed picture of the temporal and spectral characteristics of its emission. The recent analysis of the COS-B data by Clear et al., 1987 is summarized in the following section. COS-B accumulated a total exposure of $1.5 \times 10^8\ cm^2 s$ above 50 MeV in 6 observation periods spanning the time from September 1975 to March of 1982. The instrument registered about 860 photons from the pulsar and $\sim$ 900 from the unpulsed source. A pulsar lightcurve constructed from photons in the range 50-3000 MeV is shown in figure 1 with a bin size of $\sim$ 0.66 ms. The extremely narrow pulses (FWHM between 1 and 2 ms) are separated in phase by 0.39 ± 0.02, equivalent to $140° \pm 7°$. If the magnetic field in the emission region shapes the beam pattern, e.g. as would be expected in models invoking curvature radiation, the angular divergence of the field lines should be between 10° and 20° in this region.

Between the two peaks of emission, the Crab pulsar, most pronounced at X-ray energies around 100 keV, shows a so-called interpulse component. The COS-B observations revealed this interpulse component for the first time at energies above 50 MeV. One recent interpretation of the interpulse (Hasinger, 1985) in a one-pole hollow cone model puts the origin of this component into an outflow of particles over the polar cap, which radiate curvature radiation, while the main pulses are generated in a synchrotron process close to the light cylinder. This interpretation will have to be investigated in the context of apparent secular time variations of the pulsar light curve as will be presented below.

The spectrum of the pulsed radiation can be derived from the analysis of phase histograms pertaining to selected energy intervals, as shown in figure 2. The two emission peaks are clearly visible into the 800-1500 MeV range (the 'pulse-phase interval' from $\varphi = 0.1$ to 0.6 has 39 counts while the equally long 'background' interval has only 13 counts). In the highest energy band from 1.5 to 3 GeV one finds 14 'pulsed' counts vs. 5 in the 'background'. With a poisssonian probability of 5×10^{-4} this accumulation of counts is due to a chance fluctuation. It is therefore

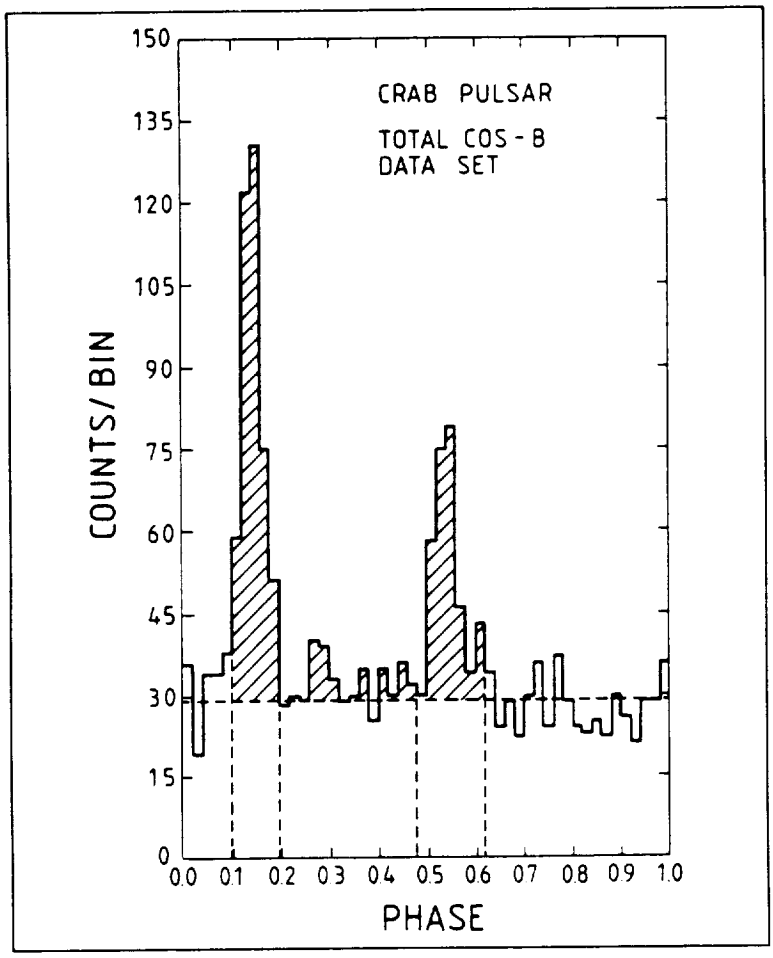

Figure 1: The Crab Pulsar lightcurve for 50 - 3000 MeV from the total COS-B data set

likely that Crab produces pulsed photons with energies in excess of 1 GeV!

Clear et al. derived the spectra for the components of the lightcurve, first-, second-, and interpulse, independently. Within statistics they found that the spectra could all be described with a power law of index $-(2.00 \pm 0.10)$ between 50 and 3000 MeV. The total spectrum is

$$\Phi(E) = (2.86 \pm 0.5) \times 10^{-4}\ E^{-2.00 \pm 0.10} \text{ photons (cm}^2 \text{ s MeV)}^{-1}$$

The average share of the first pulse is 50%, of the second 34% and of the interpulse 16%. Although we think that a significant secular variation in the ratio of the first to the second pulse is present in the SAS-2 and COS-B data, the absolute fluxes of the components during the six COS-B observations show no significant variations which exceed the large statistical and systematic uncertainties.

The unpulsed, steady emission of the Crab is derived from a comparison of 'pulsed' and 'unpulsed' skymaps of the region. A strong, steady source, contributing nearly 50% to the signal below about 500 Mev, was detected and its spectrum can be described as a power law of index -2.7. Although intensity and spectral slope of this unpulsed emission from the Crab

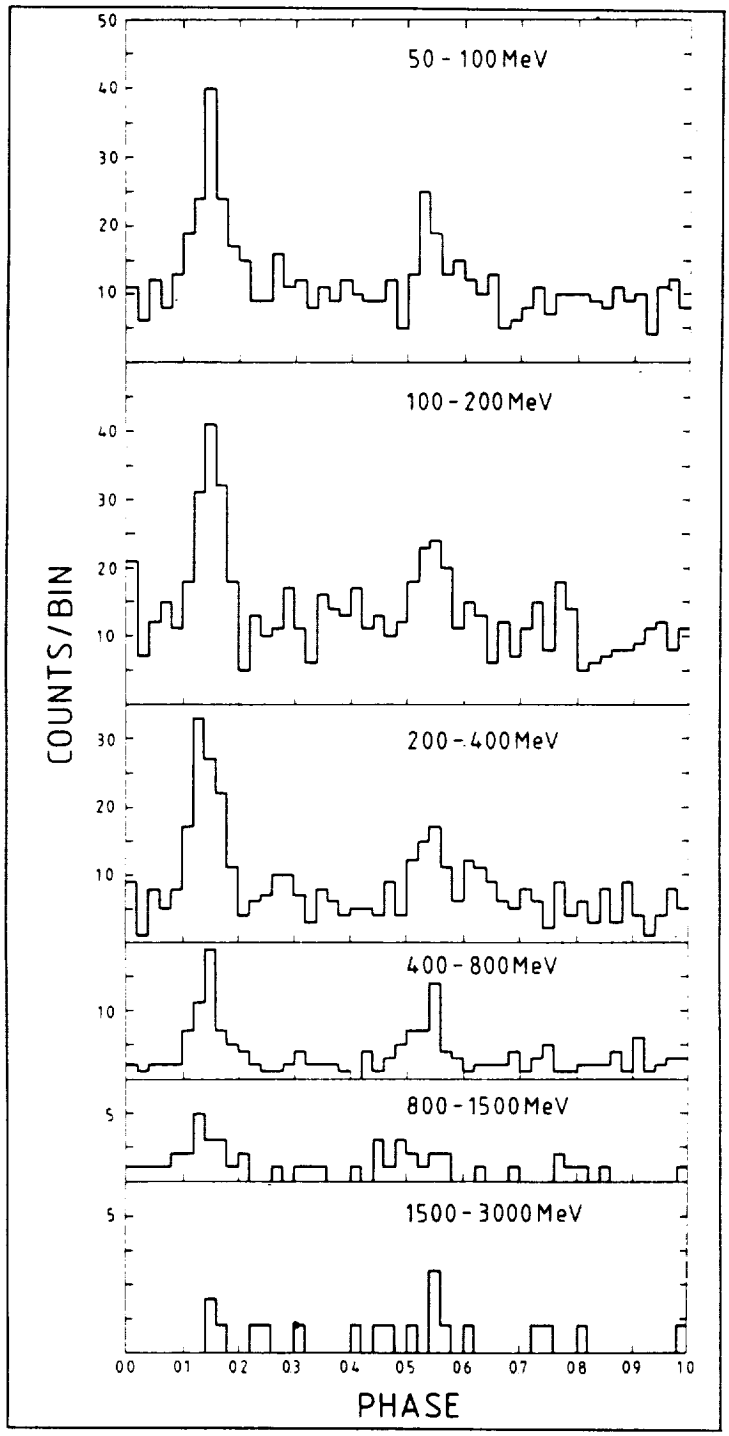

Figure 2: Crab Pulsar phase histograms for six energy bands from the total COS-B data set

is consistent with the extrapolation of the spectrum at hard X-rays, an identification of this emission with the nebula would be premature: neither at X-rays nor in the gamma energy range is the angular resolution sufficient for the separation of a possible steady flux from the neutron star and from the extended nebula.

Wills et al., 1982 observed in the COS-B Crab data a possible temporal variation in the relative count rates from the first and second pulses. Figure 3 shows the pulse ratio P_2/P_1 observed during the COS-B mission augmented by a data point from the SAS-2 observations above 35 MeV. The probability that these secular variations are due to chance fluctuations was estimated by Clear et al. to be about 1%. It should be noted that simultaneous observations of the Crab lightcurve between 2 and 6 keV from a small X-ray detector on COS-B showed no variations of this type.

Notwithstanding the scant observational evidence, it is interesting to speculate on the possibility of a periodic process that manifests itself in such a variation at gamma-ray energies: a tentative fit of the data with a sine function

$$P_2/P_1 = 0.9 - 0.5\, sin(2\pi(t - 1975.5)/14a)$$

leads to a period of about 14 years. The fit is shown in figure 3. A possible explanation could be found in a free nutation of the neutron star: Goldreich, 1970 stated:..'if circumstances exist in which the free nutation is excited, the narrow beaming of pulsar signals would make it easy to detect'. So we assume that the radiation pattern at gamma-ray energies cycles periodically with an amplitude of typically 10° (i.e. the size of a beam) and we observe changes in the relative pulse strengths due to their particular alignment.

The frequency of a free nutation Ω is proportional to differences in the principal angular momenta of a tri-axial rigid body $(I_3 - I_1)/I_1$ and to $\omega\, cos\, \alpha$, the product of the spin frequency and the cosine of the nutation amplitude. Goldreich describes two possible momenta imbalances for rotating neutron stars:

- dipole induced moment differences: $\sim 10^{-11} R_6^4 B_{12}^2 M^{-2}$
- crust rigidity induced moment differences: $\sim 10^{-11} R_6^7 \mu_{30} M^{-3} P^{-2}$

with radius R_6 (in 10^6 cm), surface magnetic field B_{12} (in 10^{12} Gauss), mass M in $M_\odot$, period P in seconds and μ_{30} is the shear modulus in units of 10^{30} dynes cm^{-2}.

For the hypothetical Crab nutation we have $\Omega/\omega\, cos\, \alpha \approx 8 \times 10^{-10}$. This is to be compared with values based on the dipole induced (magnetic stress) and rigidity induced moment differences for Crab: reasonable values of $B_{12} \approx 4$, $M \approx 1.4$ lead to $\Omega/\omega\, cos\, \alpha \approx 7 \times 10^{-11} R_6^4$ for the magnetic stress case and to $\Omega/\omega\, cos\, \alpha \approx 3 \times 10^{-9} R_6^7 \mu_{30}$ for the effect of the star's rigidity. The shear modulus for a neutron star mantle is not known, but has been estimated to $\mu_{30} \ll 1$. A most important parameter is of course the stellar radius (really the mass - radius relation, i.e. the equation of state). In spite of the unknowns, the explanation of the hypothetical nutation as a magnetic stress effect would require $R_6 \approx 1.8$, which is entirely in agreement with estimates of $R_6 = 1.6$ by Pandharipande et al., 1976. If the mechanical explanation with a rigid crust is accepted with a similar radius value, then μ_{30} should be around 10^{-2}.

The observation of nutation could clearly help in these fundamental questions of neutron star physics. With the hope that GRO might shed some light on this speculation I finish this excursion.

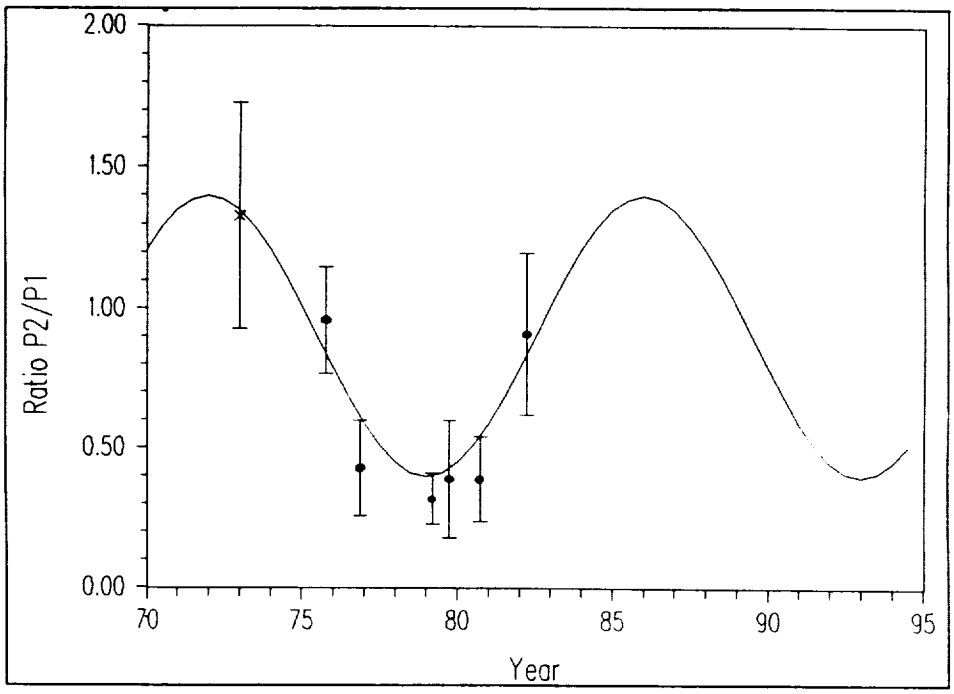

Figure 3: Secular variation of the ratio of counts in the second pulse and in the first pulse of the Crab lightcurve. The COS-B data (•) are for 50-3000 Mev, the SAS-2 point (×) (1973) for > 35 MeV. The sine function fit is discussed in the text.

III. THE VELA PULSAR

The best information presently available on the high-energy emission of PSR0833-45 is again provided by the extensive COS-B database, which contains ten relevant observations between October, 1975 and May, 1981 with a total exposure of 1.5×10^8 $cm^2 s$ between 50 MeV and 5 GeV on the source. About 3000 photons above 50 MeV and 1700 above 100 MeV were detected by COS-B from Vela and were used in a detailed analysis by Grenier, Hermsen and Clear, 1988. The EGRET instrument should be able to accumulate about three times as many photons in the course of a single 2-week observation period. Considering the richness of information on the pulsar emission processes already apparent in the COS-B data, it is quite reasonable to expect further refinements and exciting new results based on the EGRET observations; it would however also be necessary to provide for regular, repeated observations to cover the long-term variations.

Confirmed detections of the Vela pulsar have been reported at radio, optical and gamma-ray energies. A compilation of the pulse characteristics at these frequencies is shown in figure 4. At X-ray energies Vela has only been detected as a steady source but no pulsed signal has yet been found. In the analysis of the COS-B data Grenier et al. defined several phase regions of the pulsar lightcurve and named the components in sequence: Pulse 1, Interpulse-1, Interpulse-2, Pulse 2, Trailer and background as indicated in figure 4. It will be seen that these phase components show sufficiently different radiation characteristics (temporal and spectral)

to justify the assumption that we observe different physical phenomena at different phases of the pulsar period.

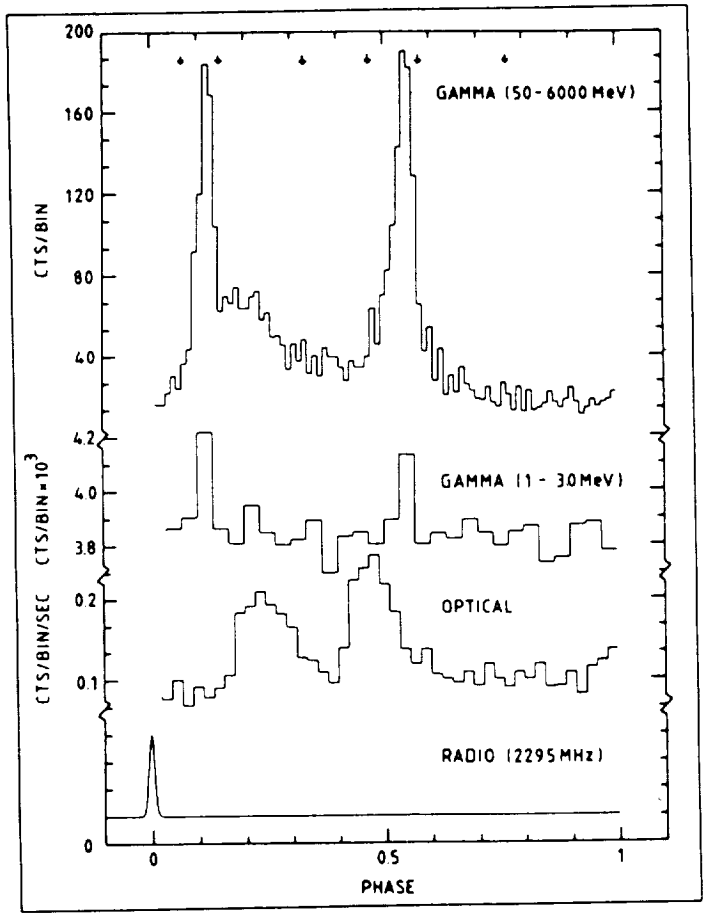

Figure 4: The Vela Pulsar lightcurves at gamma ray (50-6000 MeV, total COS-B data set, 1-20 MeV, Tümer et al., 1984) optical and radio frequencies. Phase intervals as described in the text are indicated in the high-energy histogram.

The phase separation of the pulse maxima in Vela is 0.426 ± 0.006 corresponding to an angle of $153° \pm 2°$, which is marginally larger than for the Crab pulsar. The sharpness of the pulses, in particular of the first pulse, is even more visible in a lightcurve with 0.5 ms binsize (Kanbach et al., 1980): a spike at the first pulse ($3 - 4\sigma$ excess) is contained in one phase bin. The beaming mechanism of Vela must be able to collimate parts of the emission to within a few degrees!

The gamma-ray flux from Vela turned out to be quite variable on time scales between weeks (lower limit due to counting statistics) and years. Flux differences of up to a factor of three have been detected by Grenier et al., most pronounced at lower energies. Figure 5a depicts the flux at 50 MeV - 5 GeV over the epochs of COS-B observations, while a 'zoom' with higher

time resolution is shown in figure 5b for the years 1975-78. It is tempting to associate the flux increase during the first observations with a large glitch in pulsar period and -derivative, which occured sometime between Sept. 25 and Oct. 15, 1975: with a rise-time scale of about 11 days and a decay scale of 137 days (shown as curves in figure 5b) this gamma ray flare peaked about a month after the glitch. The pulsar's energy source, the rotational braking, increases by about 1% after a glitch. Since the gamma-ray luminosity nearly doubled after the glitch and the normal gamma-ray efficiency is also about 1% we would have to conclude that nearly all of the glitch related power increase would have to be converted into high energy emission.

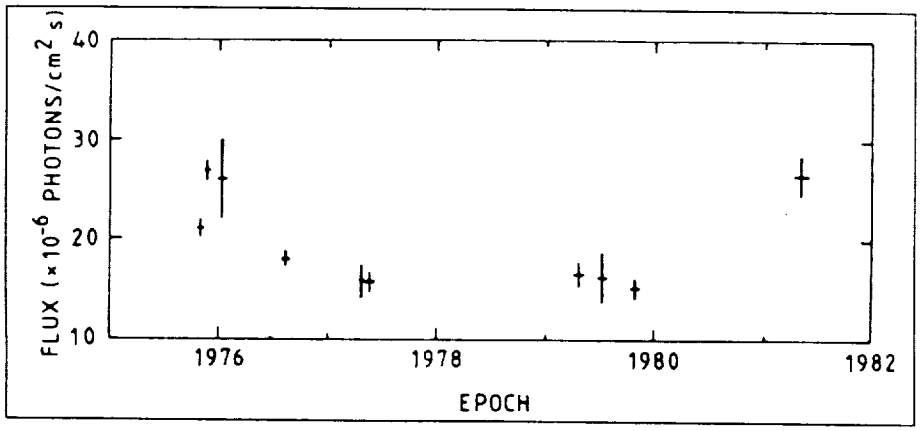

Figure 5a: Vela pulsar integrated gamma ray flux for 50-6000 MeV at epochs of COS-B observations

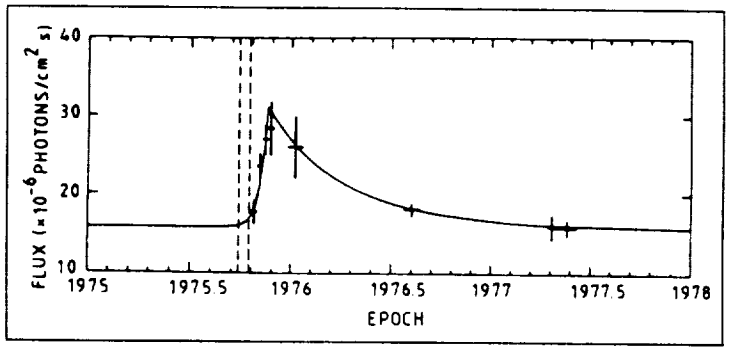

Figure 5b: Higher time resolution gamma ray flux for 50-6000 MeV

Unfortunately we have little further evidence to associate such episodes of enhanced gamma-ray luminosity with glitches in the pulsar's rotation: the next period discontinuity after the October 1975 glitch occured between June 20 and July 13, 1978. The COS-B observation nine months later during April, 1979 showed no exceptional luminosity, which is not surprising in view of the possible time-scale of a few months for a glitch related gamma flare. During the last Vela exposure of COS-B during April and May, 1981 however we find an enhanced flux without

a report of a period glitch in the preceding months. Five months later (October 1981) the next glitch occured!

This puzzle of irregular intensity variations is further complicated if one looks to other wavelengths. At radio energies, a long term variability (factor of 2 to 3 in intensity) has been observed with a rather regular time scale of a few (2.5 to 3) years. These radio intensity changes however don't seem to be related to the gamma-ray fluctuations; as a possible explanation for the radio changes McAdam, 1981 has proposed precessional effects on the beaming geometry. The relevant ratio of $\Omega/\omega \cos\alpha$ for the Vela pulsar would be about 1×10^{-9} and is therefore comparable to the value quoted above for the Crab pulsar.

The total pulsed gamma-ray spectrum, averaged over all COS-B observations of PSR0833-45, is shown in figure 6. It is evident that a single power law is insufficient to describe the spectrum from 50 to 5000 MeV. Grenier et al. derived the following fits for the radiation above and below 300 MeV:

$$F(50 \leq E \leq 300 MeV) = (2.74 \pm 0.21) \times 10^{-4} E_{MeV}^{-1.72 \pm 0.07} \text{ photons / cm}^2 \text{ s MeV}$$
$$F(300 \leq E \leq 5000 MeV) = (2.71 \pm 0.04) \times 10^{-3} E_{MeV}^{-2.12 \pm 0.07} \text{ photons / cm}^2 \text{ s MeV}$$

The intensity of the Vela pulsar allows a much more detailed analysis of the spectrum as a function of phase and epoch. As indicated in figure 4 five components have been defined in the lightcurve and the analysis of Grenier et al. showed that each component has individual characteristics as well as common features with respect to the average spectrum. A common feature of all components is the spectral index of the high energy emission above 300 MeV. Within errors the slopes of all distinct spectra agree with the average value given above. At low energies (50-300 MeV) however the pulsar varies significantly over phase and epoch.

Figure 7 (a reproduction of figure 9 in Grenier et al., 1988) shows the fits to the Vela spectra, differentiated by phase intervals, for five COS-B observation epochs with the best exposures. The maximum likelihood fits are based on two power laws between 50 - 300 MeV and 300-5000 MeV. The whole pulsed emission, in panel 7f, shows the relative stability of the pulsar above 300 MeV. At lower energies the spectral slope and intensity vary significantly. The flux variations shown in figure 5 are almost entirely due to the low energy range. The average spectrum of the first pulse is significantly softer than the spectra of interpulse-1 and pulse 2. These spectral differences and the individual variations seem to indicate that the emission in the respective phase intervals is generated by different processes and perhaps at different locations in the pulsar's magnetosphere.

The strength of a continuous, steady source coincident with the Vela pulsar was determined in a comparison of skymaps constructed for the pulsed phase intervals and for the background interval. In contrast to the Crab result no localized steady source could be found at Vela over the total energy range. The upper limit of the ratio of unpulsed to pulsed flux ranges from 6% at high energies to 9% at energies around 100 MeV. The upper limit to the integral flux above 100 MeV is thus about $9 \times 10^{-7}\ cm^{-2} s^{-1}$. Following the suggestion of Pinkau, 1970 and the estimates of Higdon and Lingenfelter, 1975 a limit to the gamma-ray emission from the Vela

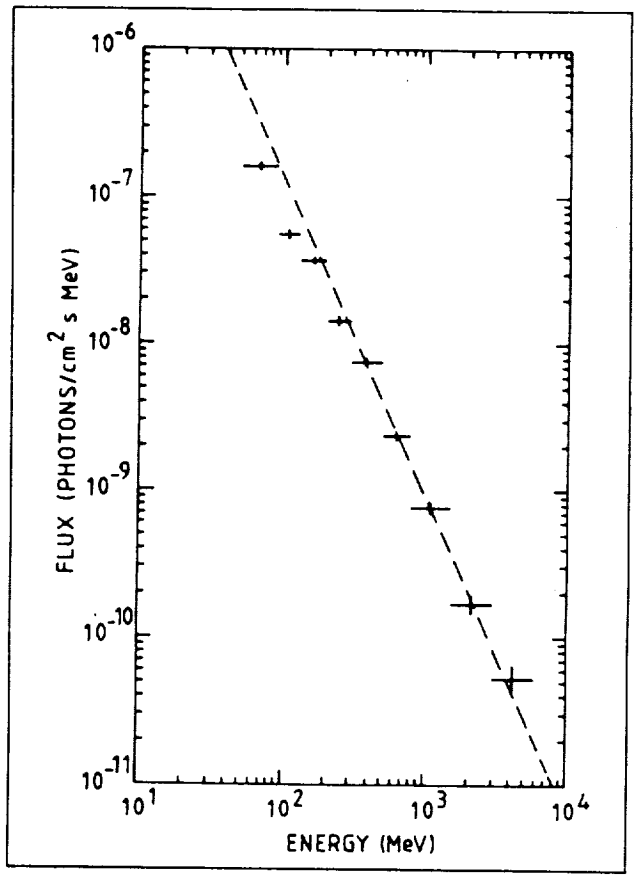

Figure 6: Differential pulsed gamma-ray spectrum of PSR0833-45 averaged over all COS-B observations. The dashed line is a fit to the data above 300 MeV

supernova remnant, and thus to the product of matter and cosmic ray density, can be derived from the quoted flux limit. We assume a matter density of 0.6 cm^{-3}, a distance of 460 pc to the remnant and a yield function of 1.4×10^{-13} $\gamma(> 100MeV)$ per second per target atom/cm^3 and per erg of cosmic ray protons an ions. The upper limit of the cosmic ray energy in the remnant is then about 2.5×10^{50} erg. Higdon and Lingenfelter estimate the requirement on the cosmic ray production in one supernova under the hypothesis that the galactic cosmic ray density is produced and maintained by supernova events which occur with a rate of one in 50 years. They find that a supernova needs to produce 3×10^{49} to 10^{50} ergs in cosmic rays. The derived limit for the Vela SNR is therefore not yet constraining this model of cosmic ray origin. Data of better statistics and definition, as expected from EGRET, might however be the basis for a new consideration of the validity of this model.

IV. CONCLUSIONS

Two of the brightest high-energy gamma-ray sources known, the Crab and Vela pulsars, have

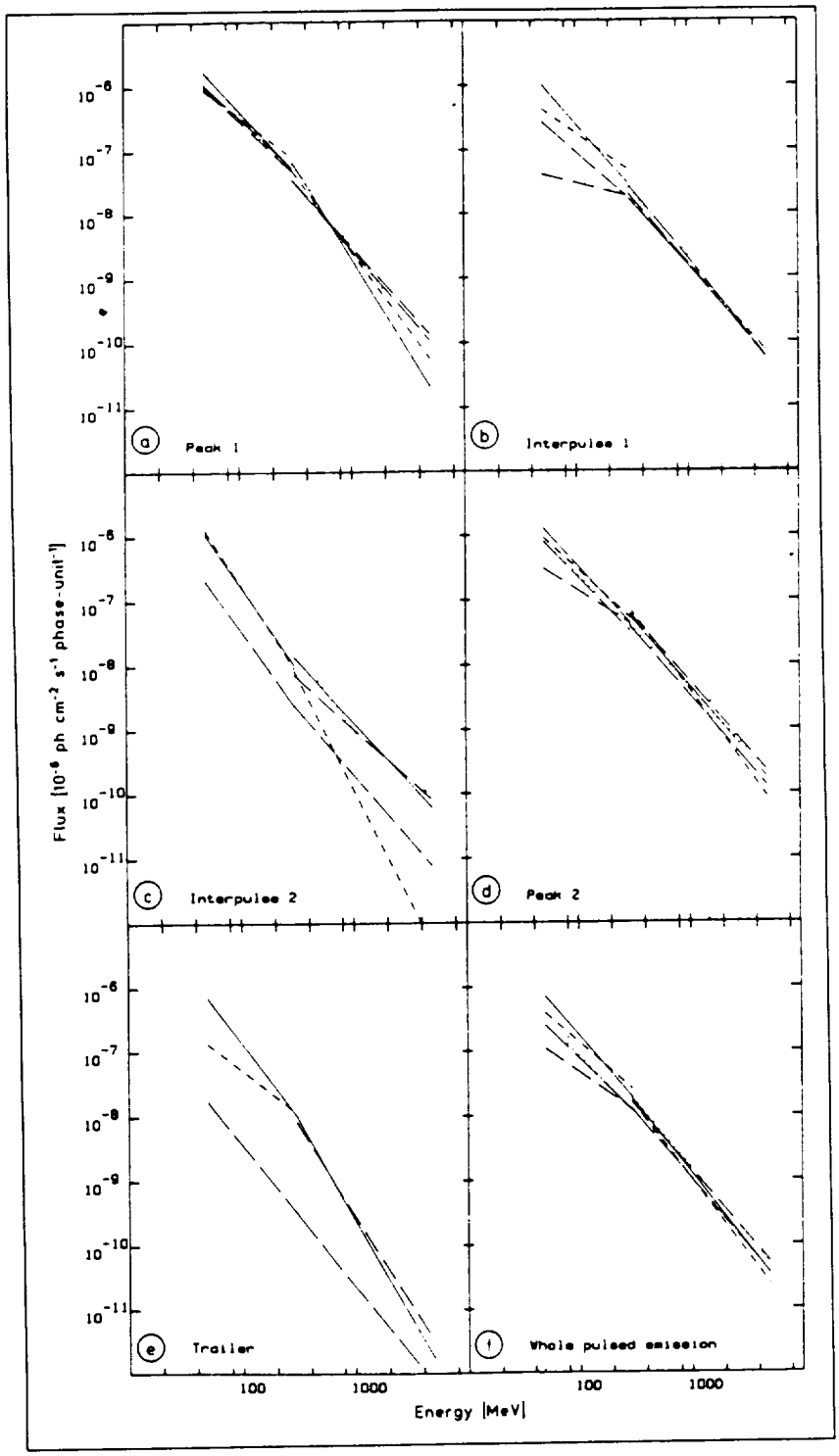

Figure 7: Differential pulsed gamma-ray spectra from PSR0833-45 for individual phase intervals and observation epochs. Maximum likelihood fits for the ranges 50-300 MeV and 300-5000 MeV are shown. For the sequence of COS-B observations refer to Grenier et al., 1988.

shown already a great wealth of temporal and spectral detail in their emission above about 50 MeV in the data from the SAS-2 and COS-B missions. Lightcurve variations over time as observed in Crab and phase dependent spectra as well as time variability in flux and spectra for Vela are indications of emission processes that are far from being understood theoretically. Progress in our understanding of these sources can certainly be obtained if we provide for GRO observations that monitor the behaviour of Crab and Vela over the total duration of the mission at regular intervals. We should further be prepared to react with GRO if unusual events are detected at other wavelengths from the young pulsars (e.g. glitches, strong variations in radio flux).

REFERENCES

Clear, J., Bennett, K., Buccheri, R., Grenier, I.A., Hermsen, W., Mayer-Hasselwander, H.A., and Sacco, B., 1987, *Astron.Astrophys.* **174**, 85.

Goldreich, P., 1970, *Astrophys.J.* **160**, L11

Grenier, I.A., Hermsen, W., and Clear, J., 1988, *Astron.Astrophys.* **204**, 117.

Hasinger, G., 1984, in M. Kafatos and R. Henry (eds.), *The Crab Nebula and Related SNRs*, Cambridge University Press, p. 47

Higdon, J.C., and Lingenfelter, R.E., 1975, *Astrophys.J.* **198**, L17.

Kanbach, G., Bennett, K., Bignami, G.F., Buccheri, R., Caraveo, P.A., D'Amico, N., Hermsen, W., Lichti, G.G., Masnou, J.L., Mayer-Hasselwander, H.A., Paul, J.A., Sacco, B., Swanenburg, B.N., and Wills, R.D., 1980, *Astron.Astrophys.* **90**, 163

McAdam, W.B., 1981, *Proc.Astr.Soc.Austr.* **4**, 219

Pandharipande,V.R., Pines, D., and Smith, R.A., 1976, *Astrophys.J.* **208**, 550.

Pinkau, K., 1970, *Phys. Rev. Letters,* **25**, 603.

Tümer, O.T., Dayton, B., Long, J., O'Neill,T., Zych, A., and White, R.S., 1984, *Nature* **310**, 214.

Wills, R.D., Bennett, K., Bignami, G.F., Buccheri, R., Caraveo, P.A., Hermsen, W., Kanbach, G., Masnou, J.L., Mayer-Hasselwander, H.A., Paul, J.A., and Sacco, B., 1982, *Nature* **296**, 723.

DISSCUSSION:

Matthew Bailes:

The efficiency of the gamma-ray production from the Vela Pulsar is often quoted as 0.01. This is dependent on the assumed distance, which is uncertain by a factor of ~2, leading to an uncertainty of ~4 in the gamma-ray efficiency.

Gottfried Kanbach:

The distance estimate is not the only uncertainty that enters the calculation of the gamma-ray efficiency of a pulsar. The moment of inertia of the rotating neutron star and the beaming geometry, i.e. the solid angle of emission are also uncertain to a similar amount. It appears however, that the 1% efficiency for Vela can be regarded as a lower limit to the conversion of rotational energy into gamma radiation.